

Basic properties of toroidal structures in Kerr–de Sitter backgrounds

Zdeněk Stuchlík and Petr Slaný

*Institute of Physics, Faculty of Philosophy and Science, Silesian University in Opava,
Bezručovo nám. 13, CZ-74601 Opava, Czech Republic*

Abstract. Perfect fluid tori with uniform distribution of the specific angular momentum orbiting the Kerr–de Sitter black holes or naked singularities are studied. Closed equipotential surfaces corresponding to stationary toroidal discs are allowed only in the spacetimes admitting stable circular geodesics. The last closed surface crosses itself in the cusp(s) enabling outflow(s) of matter from the torus due to the violation of hydrostatic equilibrium. The repulsive cosmological constant, $\Lambda > 0$, implies the existence of the outer cusp (with a stabilizing effect on the tori because of *excretion*, i.e., outflow of matter from the torus into the outer space) and the strong collimation of open equipotential surfaces along the rotational axis. Both the effects take place nearby so-called static radius where the gravitational attraction is just balanced by the cosmic repulsion. The plus-family discs (which are always corotating in the black-hole backgrounds but can be counterrotating, even with negative energy of the fluid elements, in some naked-singularity backgrounds) are thicker and more extended than the minus-family ones (which are always counterrotating in all backgrounds). If parameters of the naked-singularity spacetimes are very close to the parameters of extreme black-hole spacetimes, the family of possible disc-like configurations includes members with two isolated discs where the inner one is always a counterrotating accretion disc. Mass estimates for tori with nonrelativistic adiabatic equation of state give limits on their central mass-density, for which the approximation of test fluid is adequate.

Keywords: cosmological constant, black holes, naked singularities, toroidal structures

PACS: 04.70.Bw, 04.20.Dw, 95.30.Sf, 98.62.Mw, 98.80.Es

1. INTRODUCTION

Disc-like structures orbiting black holes seem to play an important role in a wide range of astrophysical phenomena including the most energetic processes in the Universe connected with quasars, or the formation of probably the largest disc structures at all–galactic discs. On the other hand, various cosmological observations indicate convincingly that in the framework of inflationary cosmology a non-zero, although very small, vacuum energy density, i.e., a relic repulsive cosmological constant, $\Lambda > 0$, or some similarly acting new kind of fields called *quintessence*, has to be invoked in order to explain the dynamics of the recent Universe [1, 2]. Both possibilities are often referred as a *dark energy* in the Universe. It is well known that the repulsive cosmological constant strongly influences expansion of the Universe, leading finally to an exponentially accelerated stage. The paper shows, surprisingly enough, that the repulsive cosmological constant could be relevant also in astrophysical processes like the disc accretion onto a supermassive black hole and the formation of the largest disc structures in the Universe.

Recent data from a wide variety of independent cosmological tests give the current value of the vacuum energy density to be [3]

$$\rho_{\text{vac}(0)} \approx 0.73\rho_{\text{crit}(0)}, \quad (1)$$

where the present value of the critical energy density $\rho_{\text{crit}(0)}$ is related with the Hubble parameter H_0 by¹

$$\rho_{\text{crit}(0)} = \frac{3H_0^2}{8\pi}, \quad H_0 = 100h \text{ km s}^{-1} \text{ Mpc}^{-1}. \quad (2)$$

Taking value of the dimensionless parameter $h \approx 0.7$, we obtain for the relic repulsive cosmological constant its current value

$$\Lambda_0 = 8\pi\rho_{\text{vac}(0)} \approx 1.3 \times 10^{-56} \text{ cm}^{-2}. \quad (3)$$

¹ Geometric units $c = G = 1$ are used hereafter.

Basic properties of geometrically thin (accretion) discs with low accretion rates and negligible pressure are given by the circular geodesic motion in the black-hole backgrounds [4], while for geometrically thick discs with high accretion rates and pressure being relevant they are determined by equipotential surfaces of test perfect fluid rotating in the background (see, e.g., [5]). The equipotential surfaces can be closed or open. Moreover, there is a special class of critical surfaces self-crossing in a cusp(s), which can be either marginally closed or open. The closed—toroidal—equipotential surfaces determine stationary configurations (tori). The fluid can fill any toroidal equipotential surface; at the surface of the torus pressure vanishes, but its gradient is non-zero [15]. On the other hand, the open equipotential surfaces are important in dynamical situations, e.g., in modeling of jets [20, 21], as the matter can flow along the open surfaces. The critical—marginally closed—equipotential surfaces W_{crit} are important in the theory of thick accretion discs, because accretion onto the black hole through a cusp of the equipotential surface, located in the equatorial plane, is possible due to a small overcoming of the critical surface by the surface of the disc (Paczynski mechanism). Accretion is thus driven by a violation of the hydrostatic equilibrium, rather than by viscosity of the accreting matter [15].

The equatorial circular motion of test particles (Keplerian motion) and its relevance for thin accretion discs were studied thoroughly in the case of Schwarzschild–de Sitter (SdS) geometry in [6], and in the case of Kerr–de Sitter (KdS) geometry in [7], even if some important remarks can also be found in the work of Carter or Demianski [8, 9]. It was shown that thin discs have, besides the standard inner edge at the inner marginally stable circular orbit, an outer edge at the outer marginally stable circular orbit located slightly under the static radius of the given spacetime. The static radius is an unstable circular orbit where the gravitational attraction of the black hole is just compensated by the cosmic repulsion and where the static geodesic observer, i.e., the geodesic observer with only the time-component of its 4-velocity being non-zero, resides. Moreover the accretion efficiency, $\eta = E_{\text{ms}(o)} - E_{\text{ms}(i)}$, given by the difference of the specific energies at the outer and the inner marginally stable orbits, is smaller when compared with the asymptotically flat geometries, especially due to the fact that $E_{\text{ms}(o)} < 1$.

Equilibrium toroidal configurations of barotropic perfect fluid orbiting in the Schwarzschild–de Sitter background were studied in [10]. An analysis of the structure of equipotential surfaces revealed the existence of another (outer) critical point (the so-called cusp) in which one of the equipotential surfaces is self-crossing. As the discussed equilibrium of fluid tori is the hydrostatic equilibrium, the outer cusp, when it is located on the marginally closed equipotential surface, determines the outer edge of the disc, exactly in the same way as the inner cusp determines the inner edge [15]. Moreover, the outflows through the outer cusp can stabilize the accretion discs against so-called *runaway instability* [23], as shown by Rezzolla et al. [11]. When the critical surface with the inner cusp is open or does not exist, while the critical surface with the outer cusp is marginally closed, such a configuration corresponds to a completely new type of discs called *excretion disc*. More detailed description of possible equilibrium configurations of barotropic fluid in the backgrounds with $\Lambda > 0$ is given in the Sec. 3 below where the situation is discussed in the case of KdS geometry. Strong collimation of open equipotential surfaces near the axis of rotation suggests a tendency of backgrounds with $\Lambda > 0$ to collimate streams of particles (jets) moving along the rotational axis.

Equilibrium toroidal configurations of barotropic perfect fluid orbiting in the Kerr–de Sitter background were analyzed thoroughly in [12] where also the case of naked singularities was discussed. Here we present an overview of the basic results obtained in the approximation of test discs, and add an estimation for the central mass-energy density of an adiabatic fluid for which the obtained test-fluid results are valid.

2. KERR–DE SITTER GEOMETRY

The geometry of Kerr–de Sitter spacetimes is given by the line element

$$ds^2 = -\frac{\Delta_r}{I^2 \rho^2} (dt - a \sin^2 \theta d\phi)^2 + \frac{\Delta_\theta \sin^2 \theta}{I^2 \rho^2} [adt - (r^2 + a^2) d\phi]^2 + \frac{\rho^2}{\Delta_r} dr^2 + \frac{\rho^2}{\Delta_\theta} d\theta^2 \quad (4)$$

where

$$\Delta_r = r^2 - 2Mr + a^2 - \frac{1}{3}\Lambda r^2 (r^2 + a^2), \quad \Delta_\theta = 1 + \frac{1}{3}\Lambda a^2 \cos^2 \theta, \quad I = 1 + \frac{1}{3}\Lambda a^2, \quad \rho^2 = r^2 + a^2 \cos^2 \theta. \quad (5)$$

The spacetime is specified by three parameters: central mass (M), rotational parameter (a) corresponding to the specific angular momentum of the central object, and positive cosmological constant (Λ). It is convenient to introduce the dimensionless “cosmological parameter”

$$y = \frac{1}{3}\Lambda M^2 \quad (6)$$

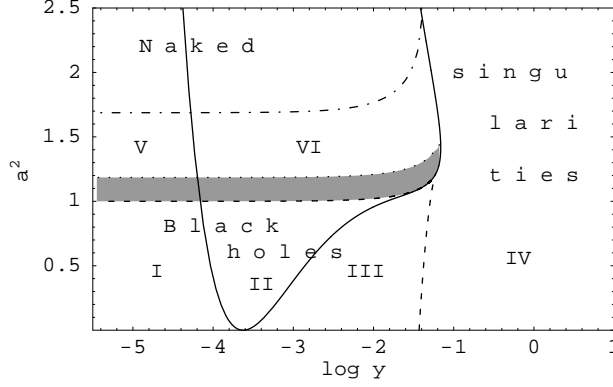


FIGURE 1. Division of KdS spacetimes according to the existence of stable equatorial circular orbits (SECOs). **(I)** Black-hole (BH) spacetimes with both direct and retrograde SECOs. **(II)** BH spacetimes with no retrograde SECOs. **(III)** BH spacetimes with no SECOs. **(IV)** Naked-singularity (NS) spacetimes with no SECOs. **(V)** NS spacetimes with both direct and retrograde SECOs. **(VI)** NS spacetimes with no retrograde SECOs. The dashed-dotted curve forms the boundary of NS region, where the retrograde plus-family SECOs exist; shaded is its subregion where such SECOs possess negative energy.

and reformulate relations (4)–(5) into the completely dimensionless form by putting $M = 1$ hereafter. The spacetime is stationary, axially symmetric and asymptotically de Sitter.

The spacetime horizons are determined by the condition $\Delta_r = 0$. In general, three horizons (the inner and the outer of the black hole, r_{h-} and r_{h+} , and the cosmological one, r_c) exist. A more detailed discussion on the existence of event horizons of KdS geometry including the extreme cases in which two or even three horizons coincide can be found in [7]. Note that cosmological horizon, behind which the geometry is dynamic, exists in all KdS spacetimes, and that there is a maximal value of the cosmological parameter allowing the existence of black holes: $y_{\text{crit}} \doteq 0.059$.

An analysis of the equatorial circular orbits of test particles in terms of the stability against radial perturbations enables to divide the parametric space (y, a^2) into six regions corresponding to the black-hole/naked-singularity spacetimes containing stable equatorial circular geodesics of a given family (Fig. 1). In the black-hole backgrounds, the plus-family corresponds to the stable corotating orbits while the minus-family to the stable counterrotating ones, where the direction of the orbits is related to the locally non-rotating frames (LNRFs) introduced by Bardeen *et al.* [13]; the orbits with locally measured azimuthal component of its 4-momentum $P^{(\phi)} > 0$ are called direct or corotating, while the ones with $P^{(\phi)} < 0$ are called retrograde or counterrotating. In the naked-singularity backgrounds, there is a sort of stable plus-family orbits which are counterrotating from the point of view of LNRFs, even with negative specific energy (the shaded region in Fig. 1). Note that also in black-hole backgrounds, contrary to the Kerr case ($y = 0$), the plus-family orbits can be both direct or retrograde, however, the retrograde ones, located near the upper limiting radius for the existence of the plus-family orbits (static radius or the retrograde photon circular orbit), are unstable. Moreover, for each family of orbits there is a maximal value of the cosmological parameter allowing the stable circular orbits of a given family: $y_{c(\text{ms}+)} \doteq 0.069$ and $y_{c(\text{ms}-)} = 12/15^4 \doteq 0.00024$; the latter coincides with the maximal value of y allowing the stable circular orbits in SdS spacetimes [6]. A detailed discussion of the direction and stability of equatorial circular orbits can be found in [7].

3. EQUIPOTENTIAL SURFACES

Analytic theory of equilibrium configurations of rotating perfect fluid bodies was developed by Boyer [14] and then studied by many authors. The main result of the theory, known as “Boyer’s condition”, states that the boundary of any stationary, barotropic, perfect fluid body has to be an equipotential surface. Here we shall summarize its application to the relativistic test perfect fluid orbiting in a stationary and axisymmetric way in a stationary, axisymmetric background, as was introduced by Abramowicz and co-workers in the case of Schwarzschild and Kerr black holes [15, 16], and use it for an analysis in the KdS spacetimes [12].

In the standard Boyer–Lindquist coordinates the spacetime is described by the line element

$$ds^2 = g_{tt}dt^2 + 2g_{t\phi}dtd\phi + g_{\phi\phi}d\phi^2 + g_{rr}dr^2 + g_{\theta\theta}d\theta^2 \quad (7)$$

satisfying the properties of stationarity and axial symmetry, i.e., $\partial_t g_{\mu\nu} = \partial_\phi g_{\mu\nu} = 0$. The stress-energy tensor of perfect fluid is given by

$$T^\mu{}_\nu = (\varepsilon + p)U^\mu U_\nu + p\delta_\nu^\mu, \quad (8)$$

where ε and p are total energy density and pressure of the fluid, respectively. Further, we consider test perfect fluid with the 4-velocity $U^\mu = (U^t, U^\phi, 0, 0)$; orbital motion of the fluid is characterized by vector fields of the angular velocity $\Omega(r, \theta) = U^\phi/U^t$ and the specific angular momentum $\ell(r, \theta) = -U_\phi/U_t$, related by the metric coefficients of the background

$$\Omega = -\frac{g_{t\phi} + \ell g_{tt}}{g_{\phi\phi} + \ell g_{t\phi}}. \quad (9)$$

The relativistic Euler equation in the axially symmetric form reads

$$\frac{\partial_i p}{\varepsilon + p} = -\partial_i(\ln U_t) + \frac{\Omega \partial_i \ell}{1 - \Omega \ell}, \quad (10)$$

where $i = r, \theta$ and

$$(U_t)^2 = \frac{g_{t\phi}^2 - g_{tt} g_{\phi\phi}}{g_{\phi\phi} + 2\ell g_{t\phi} + \ell^2 g_{tt}}. \quad (11)$$

For a barotropic fluid, i.e., for a body with an equation of state $p = p(\varepsilon)$, the surfaces of constant pressure are given by the equipotential surfaces of the potential $W(r, \theta)$ defined by the relations [16]

$$\int_0^p \frac{dp}{\varepsilon + p} = \ln(U_t)_{\text{in}} - \ln(U_t) + \int_{\ell_{\text{in}}}^\ell \frac{\Omega d\ell}{1 - \Omega \ell} \equiv W_{\text{in}} - W, \quad (12)$$

where the subscript “in” refers to the inner edge of the disc. The explicit form of the potential, $W = W(r, \theta)$, is given by the relations (11) and (12), if one specifies the metric tensor of the background and the “rotational law”, i.e., the function $\Omega = \Omega(l)$. The simplest but astrophysically very important is the case of uniform distribution of the specific angular momentum,

$$\ell(r, \theta) = \text{const}, \quad (13)$$

through the disc. It is well known that the tori with $\ell(r, \theta) = \text{const}$ are marginally stable [17] and capable to produce maximal luminosity at all [18]. Note that topological properties of the equipotential surfaces seem to be rather independent of the distribution of the specific angular momentum $\ell(r, \theta)$, see, e.g., [18, 19, 5]. In this special case the potential is given by very simple formula

$$W(r, \theta) = \ln U_t(r, \theta). \quad (14)$$

The points where $\partial_r W = 0$ correspond to free-particle (geodesic) motion due to the vanishing of the pressure-gradient forces there. Moreover, at the center of any perfect fluid torus the pressure attains the extreme value (maximum) and matter must follow a stable geodesic there. Thus, thick discs can exist only in the backgrounds allowing the motion along stable circular geodesical orbits.

In the KdS backgrounds, the potential (14) takes the form

$$W(r, \theta) = \ln \left\{ \frac{\rho^2}{I^2} \frac{\Delta_r \Delta_\theta \sin^2 \theta}{\Delta_\theta (r^2 + a^2 - a\ell)^2 \sin^2 \theta - \Delta_r (\ell - a \sin^2 \theta)^2} \right\}^{1/2}. \quad (15)$$

Performing the limit $a \rightarrow 0$, we get the corresponding form of the potential (14) in the SdS backgrounds [10]. All relevant properties of the equipotential surfaces are determined by the behaviour of the potential in the equatorial plane ($\theta = \pi/2$). Inspecting the reality conditions of $W(r, \theta = \pi/2)$ in the stationary parts of the background ($\Delta_r \geq 0$; in the black-hole backgrounds, we restrict our attention to the stationary region between the (outer) black-hole and cosmological horizon only), we arrive at the condition for the occurrence of matter with a given distribution of $\ell(r, \theta)$,

$$\ell_{\text{ph-}} < \ell < \ell_{\text{ph+}}, \quad (16)$$

where

$$\ell_{\text{ph}\pm}(r; a, y) = a + \frac{r^2}{a \pm \sqrt{\Delta_r}} \quad (17)$$

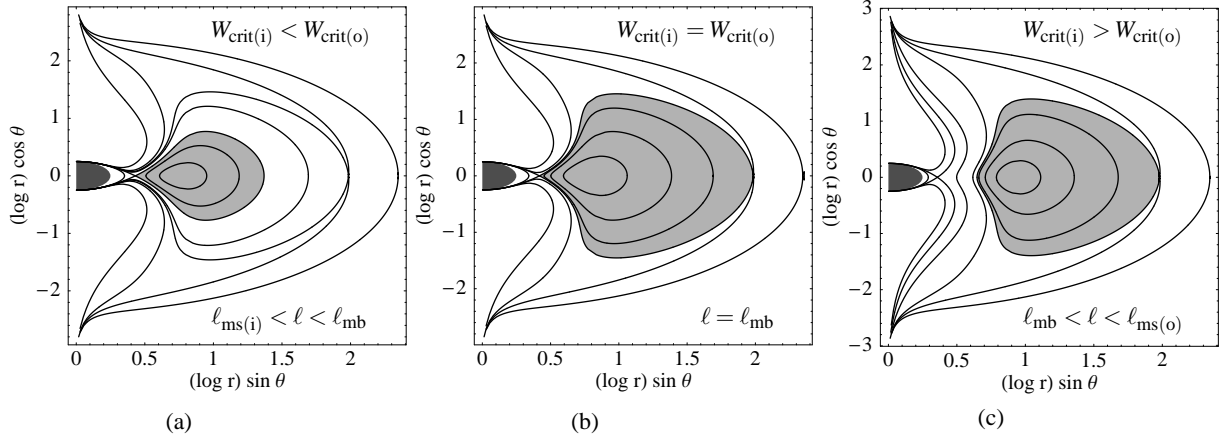


FIGURE 2. Typical behaviour of equipotential surfaces (meridional sections) in SdS and KdS black-hole spacetimes. Light gray region contains closed equipotential surfaces. The last closed surface is self-crossing in the cusp(s). Possible toroidal configurations correspond to: (a) accretion discs, (b) marginally bound accretion discs and (c) excretion discs. (The figures are drawn for the KdS spacetime with $y = 10^{-6}$, $a^2 = 0.6$ using the standard Boyer-Linquist coordinates.)

corresponds to the effective potential of the photon geodesic motion; see [22] for an alternative definition. Local extrema of the function $W(r, \theta = \pi/2)$ lie at those radii where the specific angular momentum coincides with the specific angular momentum of test particles moving on the geodetical (Keplerian) circular orbits, i.e., where

$$\ell = \ell_{K\pm}(r; a, y) \equiv \pm \frac{(r^2 + a^2)(1 - yr^3)^{1/2} \mp ar^{1/2}[2 + r(r^2 + a^2)y]}{r^{3/2}[1 - (r^2 + a^2)y] - 2r^{1/2} \pm a(1 - yr^3)^{1/2}}. \quad (18)$$

Those extrema are the only local extrema of the function $W(r, \theta)$.

Toroidal configurations arise for such a distribution of $\ell(r, \theta)$ in the disc which intersects the Keplerian distribution $\ell_{K\pm}(r)$ in the part(s) corresponding to stable circular orbits. In black-hole backgrounds, stationary toroidal configurations exist for $\ell \in (\ell_{ms(i)}, \ell_{ms(o)})$, where $\ell_{ms(i)}$ ($\ell_{ms(o)}$) corresponds to the Keplerian specific angular momentum on the inner (outer) marginally stable orbit. The same is true also in most of the naked-singularity backgrounds, however, exceptions exist concerning the plus-family discs in naked-singularity backgrounds with the rotational parameter low enough to admit counterrotating stable plus-family circular geodesics, see Fig. 1. In fact, there are naked-singularity backgrounds, in which the stationary tori exist for any uniform distribution of $\ell(r, \theta)$ in the disc [12].

In both black-hole and naked-singularity backgrounds we can distinguish three kinds of discs (Figure 2):

accretion discs: Toroidal equipotential surfaces are bounded by the marginally closed critical equipotential surface self-crossing in the inner cusp and enabling outflow of matter from the disc into the BH/NS. Another critical surface self-crossing in the outer cusp is open. Matter filling the region between the critical surfaces cannot remain in hydrostatic equilibrium and contributes to the accretion flow along the inner cusp and a throat formed by open surfaces. Moreover, if the potential levels corresponding to the critical surfaces are comparable, i.e., $W_{crit(i)} \lesssim W_{crit(o)}$, huge overfilling of the critical surface with the inner cusp causing the accretion could be combined with the so-called *excretion*, i.e., outflow through the outer cusp (after overfilling of the critical surface with the outer cusp), having a capability to regulate the accretion.

marginally bound accretion discs: Such configurations exist only for the uniform distribution of the specific angular momentum in the disc $\ell(r, \theta) = \ell_{mb}$, where ℓ_{mb} corresponds to the Keplerian specific angular momentum on the marginally bound circular orbit. Toroidal equipotential surfaces are bounded by the marginally closed critical equipotential surface self-crossing in both the cusps. Any overfilling of the critical surface causes the accretion inflow through the inner cusp as well as the excretion outflow through the outer cusp.

excretion discs: Toroidal equipotential surfaces are bounded by the marginally closed critical equipotential surface self-crossing in the outer cusp and enabling outflow of matter from the disc into the outer space by a violation of hydrostatic equilibrium. The equipotential surface with the inner cusp, if such a surface exists, is open (cylindrical) and separated from the critical surface with the outer cusp by other cylindrical surfaces which, in fact, disable accretion into the black hole.

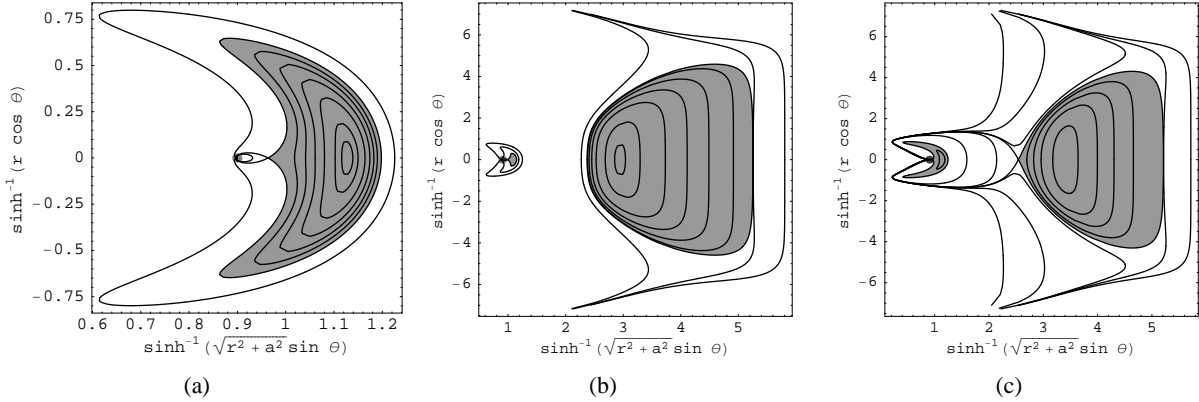


FIGURE 3. Examples of “exotic” toroidal configurations (meridional sections through the equipotential surfaces) in KdS naked-singularity spacetimes. Shaded regions contain closed equipotential surfaces. The last closed surface is self-crossing in the cusp(s). (a) Counterrotating negative-energy accretion disc. (b) Two isolated discs – the inner one is a counterrotating accretion disc, the outer one is a corotating excretion disc. (c) Two isolated discs – the inner one is a counterrotating accretion disc, the outer one is a marginally bound counterrotating accretion disc. (The figures are drawn for NS spacetimes with $y = 10^{-6}$, $a^2 = 1.05$ and the values of ℓ being equal to 8, 3.5 and -4.72 , respectively. The Kerr–Schild coordinates, covering the whole range of the disc including the ring singularity, and their appropriate scaling are used.)

In KdS naked-singularity backgrounds allowing counterrotating stable plus-family circular orbits (Fig. 1), some more exotic configurations exist:

a. counterrotating negative-energy discs

Specific energy of the fluid elements in the center and the cusps (where the fluid follows the geodesic motion) is negative and we can expect that every fluid element in the disc has energy $E < 0$. Moreover, no open equipotential surfaces going out from the singularity are connected with such configurations. In the case of accretion discs, the equipotential surface with the outer cusp need not exist (Fig. 3a).

b. configurations with two isolated discs corresponding to the same value of ℓ

The inner disc is always counterrotating accretion disc (with matter in the states with $E < 0$ or $E > 0$), the outer disc can be, in dependence on the value of ℓ , the corotating or counterrotating excretion disc, as well as the counterrotating accretion disc (Figs. 3b, c).

Due to the existence of non-zero pressure-gradients in the fluid, the inner edge of accretion discs (corresponding to the inner cusp of equipotential surfaces) is shifted under the inner marginally stable circular orbit up to the inner marginally bound circular orbit, $r_{\text{mb}(i)} < r_{\text{in}} < r_{\text{ms}(i)}$. Similarly, the outer edge of excretion discs (corresponding to the outer cusp of equipotential surfaces) is located between the outer marginally stable and outer marginally bound circular orbit, $r_{\text{ms}(o)} < r_{\text{out}} < r_{\text{mb}(o)}$. Marginally bound accretion discs have, thus, naturally determined both edges by the location of the cusps of the only critical surface, $r_{\text{in}} \approx r_{\text{mb}(i)}$, $r_{\text{out}} \approx r_{\text{mb}(o)}$, and correspond to maximally extended discs. Moreover, potential difference between the boundary (determined by the marginally closed critical surface) and the center of the torus, $\Delta W = W_{\text{crit}} - W_{\text{center}}$, takes the largest values for plus-family marginally bound accretion discs. In black-hole backgrounds, the maximal value corresponds to the disc corotating the extreme Kerr black hole ($y = 0$), $\Delta W \approx 0.549$ [16], and with the cosmological parameter y growing up to $y_{\text{crit}} \doteq 0.059$ tends to zero. In naked-singularity backgrounds, the potential difference grows unlimitedly, $\Delta W \rightarrow \infty$, for the plus-family discs orbiting a naked singularity approaching the extreme-hole state, independently of the cosmological parameter $y < y_{\text{crit}}$.

4. MASS ESTIMATES OF ADIABATIC TORI

The total mass of the disc, m , is given by the Tolman’s formula [15]

$$m = \int_{\text{disc}} \left(-T_t^t + T_r^r + T_\theta^\theta + T_\phi^\phi \right) \sqrt{-g} dr d\theta d\phi \quad (19)$$

TABLE 1. (Upper part) Mass parameter, the static radius and radius of the outer marginally stable orbit in extreme KdS black-hole spacetimes with the current value of the cosmological constant, $\Lambda_0 \approx 1.3 \times 10^{-56} \text{ cm}^{-2}$. (Lower part) Central mass-density of an adiabatic fluid for which the total mass of the disc is comparable with the mass of the SdS black hole for two values of adiabatic index $\gamma = 5/3$ and $\gamma = 7/5$.

y	10^{-44}	10^{-42}	10^{-34}	10^{-30}	10^{-28}	10^{-26}	10^{-22}
M/M_\odot	10	100	10^6	10^8	10^9	10^{10}	10^{12}
r_s /[kpc]	0.2	0.5	11	50	110	230	1100
r_{ms} /[kpc]	0.15	0.3	6.7	31	67	150	670
$\rho_c^{(5/3)}$ /[kg m^{-3}]				10^{-25}	10^{-23}		
$\rho_c^{(7/5)}$ /[kg m^{-3}]				10^{-17}	10^{-16}		

where $g = \det(g_{\mu\nu})$ and T_ν^μ is the stress-energy tensor of perfect fluid given by the relation (8). Assuming an adiabatic equation of state for a barotropic perfect fluid [24]

$$p = K\rho^\gamma, \quad \gamma = 1 + \frac{1}{n} \quad (20)$$

where γ is an adiabatic index, and a non-relativistic limit with $p \ll \varepsilon \approx \rho$, where ρ is the rest-mass density, the relation (19) can be written in an approximative form [15]

$$m = 2\pi\rho_c \int_{\text{disc}} \left[\frac{1 + \ell\Omega(r, \theta)}{1 - \ell\Omega(r, \theta)} \right] \left[\frac{W_{\text{in}} - W(r, \theta)}{W_{\text{in}} - W_c} \right]^n (r^2 + a^2 \cos^2 \theta) \sin \theta \, dr \, d\theta \quad (21)$$

in which the functions $\Omega(r, \theta)$ and $W(r, \theta)$ are given by the relations (9) and (15). W_c and ρ_c correspond to the potential value and the rest-mass density in the centre of the disc, respectively.

Comparing the total mass of the disc m with the mass of the black hole M , i.e. $m \approx M$, we can get the maximal value of the central mass-density for which the approximation of test fluid is valid in the sense $m \ll M$. The first results of numerical integration have been obtained for marginally bound accretion discs orbiting in the SdS background and for two principal values of adiabatic index $\gamma = 5/3$ and $\gamma = 7/5$. The results are presented in Table 1.

5. CONCLUSIONS

We conclude that there are two features in the structure of equipotential surfaces near the static radius of a given space-time connected with a cosmic repulsion; both have already been known from the previous analysis of equipotential surfaces in SdS backgrounds [10]. The first one is the outer cusp which enables the outflow of matter from the new type of stationary tori—the *excretion discs*. However, the outer cusp plays an important role also for the accretion discs, as puts an upper limit on their extension. Recall that no such an outer edge is naturally defined in the case of accretion discs orbiting a single black hole (naked singularity) in asymptotically flat Schwarzschild or Kerr backgrounds. The second feature connected with the cosmic repulsion consists in strong collimation of open equipotential surfaces near the axis of rotation, being evident nearby and behind the static radius, when compared with the Kerr case, see [12] for an illustrative figure, suggesting a certain role of $\Lambda > 0$ in the collimation of jets far away from the maternal accretion or excretion disc. Rotation of the background influences the shape of tori: the corotating discs are thicker and more extended than the discs in corresponding SdS background, generating a narrower funnel where the jets are most probably created [25]. On the other hand, the same is true for the discs in SdS backgrounds when these are compared with counterrotating discs in corresponding KdS background.

Finally, we shall give an idea on scales, at which the discussed effects take place, by expressing basic characteristics of the tori in astrophysical units for the current value of the cosmological constant, $\Lambda = \Lambda_0$. The results are presented in Table 1. As the outer edge of tori is located between the outer marginally stable orbit and the static radius, $r_{\text{ms}(o)} < r_{\text{out}} < r_s$, the repulsive cosmological constant puts a limit on maximal extension of disc-like structures in a given background. Remarkably for supermassive black holes ($10^6 M_\odot$ – $10^{10} M_\odot$), the dimensions of *test* tori are roughly comparable with the dimensions of galaxies [26]. The upper limits on the central mass-density of the adiabatic tori orbiting supermassive SdS black holes (10^8 – $10^9 M_\odot$), for which the test-fluid approximation is valid, are in the case

of adiabatic index $\gamma = 7/5$ one or two orders higher than the typical density of molecular clouds 10^{-18}kg m^{-3} [26]. Of course, to get a more realistic picture, influence of the cosmic repulsion on self-gravitating tori has to be studied. On the other hand, since the jets escaping from AGN can many times exceed the dimension of the galaxy, repulsive cosmological constant could play an important role in the collimation of jets far away from the “seed” galaxy.

ACKNOWLEDGMENTS

This work was supported by the Czech grant MSM 4781305903.

REFERENCES

1. N. Bahcall, J. P. Ostriker, S. Perlmutter, and P. J. Steinhardt, *Science* **284**, 1481–1488 (1999).
2. E. W. Kolb, and M. S. Turner, *The Early Universe*, Addison-Wesley, Redwood City, California, 1990.
3. D. N. Spergel, L. Verde, H. V. Peiris, E. Komatsu, M. R.olta, C. L. Bennett, and et al., *Astrophys. J. Suppl.* **148**, 175 (2003).
4. I. D. Novikov, and K. S. Thorne, “Black Hole Astrophysics,” in *Black Holes*, edited by C. D. Witt, and B. S. D. Witt, Gordon and Breach, New York–London–Paris, 1973, p. 343.
5. M. A. Abramowicz, “Physics of black hole accretion,” in *Theory of Black Hole Accretion Disks*, edited by M. A. Abramowicz, G. Björnsson, and J. E. Pringle, Cambridge University Press, Cambridge, 1998, pp. 50–60.
6. Z. Stuchlík, and S. Hledík, *Phys. Rev. D* **60**, 044006 (15 pages) (1999).
7. Z. Stuchlík, and P. Slaný, *Phys. Rev. D* **69**, 064001 (2004).
8. B. Carter, “Black Hole Equilibrium States,” in *Black Holes*, edited by C. D. Witt, and B. S. D. Witt, Gordon and Breach, New York–London–Paris, 1973, p. 57.
9. M. Demianski, *Acta Astronom.* **23**, 197 (1973).
10. Z. Stuchlík, P. Slaný, and S. Hledík, *Astronomy and Astrophysics* **363**, 425–439 (2000).
11. L. Rezzolla, O. Zanotti, and J. A. Font, *Astronomy and Astrophysics* **412**, 603 (2003).
12. P. Slaný, and Z. Stuchlík, *Classical Quantum Gravity* **22**, 3623–3651 (2005).
13. J. M. Bardeen, W. H. Press, and S. A. Teukolsky, *Astrophys. J.* **178**, 347–369 (1972).
14. R. H. Boyer, *Proc. Cambridge Phil. Soc.* **61**, 527 (1965).
15. M. Kozłowski, M. Jaroszyński, and M. A. Abramowicz, *Astronomy and Astrophysics* **63**, 209–220 (1978).
16. M. A. Abramowicz, M. Jaroszyński, and M. Sikora, *Astronomy and Astrophysics* **63**, 221 (1978).
17. F. H. Seguin, *Astrophys. J.* **197**, 745 (1975).
18. M. A. Abramowicz, M. Calvani, and L. Nobili, *Astrophys. J.* **242**, 772 (1980).
19. M. Jaroszyński, M. A. Abramowicz, and B. Paczyński, *Acta Astronom.* **30**, 1 (1980).
20. D. Lynden-Bell, *Nature* **223**, 690 (1969).
21. R. D. Blandford, “Astrophysical black holes,” in *Three hundred years of gravitation*, edited by S. W. Hawking, and W. Israel, Cambridge University Press, Cambridge, 1987, p. 277.
22. Z. Stuchlík, and S. Hledík, *Classical Quantum Gravity* **17**, 4541–4576 (2000).
23. M. A. Abramowicz, M. Calvani, and L. Nobili, *Nature* **302**, 597 (1983).
24. R. F. Tooper, *Astrophys. J.* **142**, 1541–1562 (1965).
25. J. Frank, A. King, and D. Raine, *Accretion Power in Astrophysics*, Cambridge University Press, 2002, 3rd edition.
26. B. W. Carroll, and D. A. Ostlie, *An Introduction to Modern Astrophysics*, Addison-Wesley, Reading, Massachusetts, 1996.